LCLS X-RAY PULSE DURATION MEASUREMENT USING THE STATISTICAL FLUCTUATION METHOD*

J. Wu[1†], Y. Ding[1], P. Emma[1], Z. Huang[1], H. Loos[1], M. Messerschmidt[1],
E. Schneidmiller[2], M. Yurkov[2], [1]SLAC, Menlo Park, USA, [2]DESY, Hamburg, Germany

Abstract

For a Self-Amplified Spontaneous Emission (SASE) Free-Electron Laser (FEL), the FEL pulse energy fluctuates from shot to shot, because the lasing process starts up from shot noise. When operating in the exponential growth regime, the radiation exhibits the properties of completely chaotic polarized light. Hence, the probability distribution of the FEL pulse energy follows a Gamma-distribution. Measuring such a distribution function, one can calculate the average number of "degrees of freedom" or "modes" in the radiation pulse. Measuring the FEL power gain length, one can extract the temporal duration of a single coherent spike, therefore, one can calculate the FEL pulse temporal duration. In this paper, we report experimental results at LCLS. Measurements are conducted for both nominal charge (250 pC) and low charge (40 pC and 20 pC) cases.

Introduction

It is well-known that noise can be used to infer properties of physical systems. Noise by nature carries information without disturbing its system, in contrast to externally applied diagnostics, which often modify the very parameter to be measured. Fluctuation-based diagnostic techniques have been pursued in diverse applications [1]. It has been shown that longitudinal and transverse phase space information can be obtained from a statistical analysis of fluctuations in the incoherent radiation spectrum of an electron bunch [2]. The analysis of intensity fluctuations of the SASE radiation in the high gain exponential growth regime can be used to predict the FEL pulse temporal duration [3, 4]. We report results of using this approach at the LCLS [5] to measure the FEL temporal pulse duration.

Review of the Theory

The theory is discussed in details in Ref. [6, 7], and we briefly review it here. For a SASE FEL, the FEL pulse energy fluctuates from shot to shot, because the lasing process starts up from shot noise. When operating in the exponential growth regime, the radiation exhibits the properties of completely chaotic polarized light. Hence, the probability distribution of the FEL pulse energy $p(E)$ follows

$$p(E) = \frac{M^M}{\Gamma(M)} \left(\frac{E}{\langle E\rangle}\right)^{M-1} \frac{1}{\langle E\rangle} \exp\left(-M\frac{E}{\langle E\rangle}\right), \quad (1)$$

the Gamma-distribution, where E is the FEL pulse energy, $\langle E\rangle$ is the average value of E, M is the "degrees of freedom" or "modes", and $\Gamma(x)$ is the Gamma-function. Notice that $p(E)$ is normalized, $\int_0^\infty p(E)dE = 1$.

Operating in the linear exponential regime, the FEL spectrum rms bandwidth is [8, 9]

$$\sigma_\omega(z) = \omega_r\sqrt{3\sqrt{3}\rho_{3\mathrm{D}}/(k_w z)}, \quad (2)$$

where z is the magnetic length from the undulator entrance, $k_w = \lambda_w/(2\pi)$ with λ_w being the undulator period, $\omega_r = k_r c$ with c being the speed of light in vacuum, $k_r = 2\pi/\lambda_r$ with λ_r being the FEL wavelength, and $\rho_{3\mathrm{D}}$ is introduced via the 3-D power gain length,

$$L_G^{3\mathrm{D}} = \lambda_w/(4\sqrt{3}\pi\rho_{3\mathrm{D}}). \quad (3)$$

The mode or spike temporal duration is defined as [6]

$$\tau_{\mathrm{spike}}(z) = \sqrt{\pi}/\sigma_\omega(z), \quad (4)$$

which should be viewed as the Full-Width Half-Maximum (FWHM) duration of the spike.

The FEL pulse temporal FWHM duration is then

$$\tau_{\mathrm{FEL}} = M\tau_{\mathrm{spike}}. \quad (5)$$

Notice that the theory outlined above was developed for coasting electron beam in 1-D limit. In reality, the electron bunch is not uniform in 6-D phase space, so, the FEL pulse duration can be different from the electron bunch length.

Before describing the details of the experiment, we outline the procedure here. We first measure the FEL power gain length $L_G^{3\mathrm{D}}$. Then we can compute [1] the FEL spectrum rms bandwidth $\sigma_\omega(z)$ as a function of the magnetic length z with Eqs. (2) and (3). The spike temporal duration τ_{spike} is then computed via Eq. (4). We record large number of FEL pulse energy data, and fit the data to a Gamma-distribution [2] according to Eq. (1) to find out the "degree of freedom" or the "mode" number M. Thus, the FEL pulse temporal FWHM duration τ_{FEL} is obtained according to Eq. (5).

Experiments: Nominal Charge (250 pC)

An Example The theory is valid in the linear exponential growth regime [6], hence in the measurement we use fewer undulator segments to be in the exponential regime before saturation, even though we also take data for post

* Work supported by U.S. Department of Energy, Office of Basic Energy Sciences, under Contract DE-AC02-76SF00515
† jhwu@SLAC.Stanford.EDU

[1] Of course, one can measure the FEL spectrum bandwidth directly.
[2] Indeed, how well the FEL energy fluctuation data fits to a Gamma-distribution is a measure of how small the additional fluctuation from other sources of jitter is.

Table 1: Predicted Modes Number for Peak Current Binning for 250 pC Charge with 3 kA Mean Peak Current

Number of modes	45	47	47	43	41	35
Peak current bin range (Amp)	± 15	± 30	± 45	± 75	± 150	± 300
Measurement event number within the bin	315	638	1028	1867	3388	7428

saturation regime for comparison. Let us first describe an example in details. For this example, we have a total of 28000 consecutive FEL pulse energy measurements taken at a 60-Hz single bunch repetition rate. A typical undulator setting is shown in Fig. 1 where only 15 segments (9 - 23) are inserted with each segment having 110 undulator periods of $\lambda_w = 0.03$ m. Notice also that, the undulator tapering is to compensate for the electron energy loss due to the spontaneous undulator emission, undulator vacuum chamber wakefield, and additional linear tapering of -10 MeV for segments (9-23) for FEL gain. For this measurement, the electron bunch is 'under-compressed', stopping short of the minimum possible bunch length. The electron centroid energy is 14 GeV, which produce 8.71 keV FEL with $\lambda_r = 1.42$ Å, BC2 peak current is set at 3 kA, and the charge is nominal charge of 250 pC. For this setup, the FEL power gain length $L_G^{3D} \approx 3.3$ m, so these 15 segments are about 15 power gain length. With these 15 segments, the FEL energy is about 0.3 mJ, which is about one-order of magnitude lower than the FEL saturation energy of about 2 mJ with all the undulator segments (1-23) inserted.

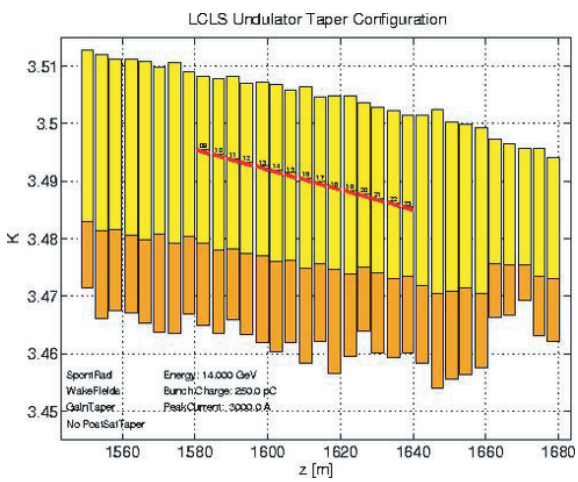

Figure 1: Typical setup of the undulator during the measurements. Vertical axis is for the undulator K value and horizontal axis is for the absolute distance from the start of the LCLS machine. The yellow band is the allowed operating range of the K value.

With the electron bunch under-compressed, the temporal distribution is expected to have a flat top in the central part with density spikes at head and tail. For electron bunch charge of 250 pC, peak current setting at 3 kA, and taking a flat-top distribution function, the electron bunch temporal rms duration is $\sigma_{t,\mathrm{ele}} = 24$ fs.

The FEL energy is measured by gas detectors with photomultiplier tubes (*e.g.*, GDET1:PMT241 as in Fig. 2), which is calibrated against electron centroid energy loss measured at the final dump magnet. The FEL pulse energy strongly depends on the electron bunch peak current, the centroid energy, and the trajectory in the undulator. Hence, we bin these three fluctuating quantities to extract the true FEL fluctuations, which will determine the true "degree of freedom" or the "modes" number in the FEL pulse. In fact, there is high correlation among the peak current, the centroid energy, and the trajectory.

As an example of binning for the peak current, in Table 1, we show the modes number as a function of the half bin size of the peak current with fixed bin size for both the electron energy centroid deviation and the trajectory. For example, for a bin size of 90 Amp, *i.e.*, $I_{pk} = 3000 \pm 45$ Amp, the measurement predicts 47 modes in the FEL pulse. When the bin size is too large, jitter induced FEL pulse energy fluctuation increases the fluctuation, and so looks like less modes in the FEL pulse. Shown in Table 1, when the bin size is 600 Amp (*i.e.*, ± 300 Amp), the FEL pulse energy fluctuation is larger and gives only 35 modes. With the decreasing of the bin size, the modes number reaches a limit of 47. Yet, when the bin size is too small, the total events number in the bin becomes too small, so fluctuation due to too few events number starts to affect the results. Shown in Table 1, when the bin size reduces to 30 Amp (*i.e.*, ± 15 Amp), the total events in this bin is only 315, and the modes number fluctuates again. So, 47 modes is roughly the number of modes in the FEL pulse. We do the same exercise for binning the centroid energy deviation and the trajectory in the undulator. By trial-and-error, we find the final bin size to be ± 45 Amp for peak current, $\pm 4.2 \times 10^{-4}$ for the electron bunch relative centroid energy deviation, which should be compared to the FEL parameter $\rho_{3D} = 4.2 \times 10^{-4}$, and ± 10 μm for the trajectory deviation at undulator segment 10. Within this bin, there are 1028 measurement events as shown in Table 1. Detailed distribution of FEL energy and peak current of these 1028 events is shown in Fig. 2. Similar plots for the FEL energy and the centroid relative energy deviation, and that for FEL energy and the x-position deviation at the undulator segment 10 are found. We want to point out that more theoretical understanding of the proper bin size is still yet to be developed. As a simple requirement, there should be no correlation between the FEL pulse energy and the quantity being binned within the final bin which is seen in Fig. 2.

The probability distribution $p(E)$ as function of the FEL energy is shown in Fig. 3, which fitting to a Gamma-function following Eq. (1) gives $M = 47$. For the

Table 2: Predicted Modes Number and FEL Pulse Temporal Duration at Different Location of the Undulator

	Undercompression			Overcompression		
Undulator Numbers	8-23	4-23	1-23	8-23	4-23	1-23
Modes Numbers	19	33	62	21	27	61
Spike Duration $\tau_{\rm spike}$ (as)	297	332	356	297	332	356
FEL Pulse FWHM temporal duration $\tau_{\rm FEL}$ (fs)	5.6	11.0	22.1	6.2	9.0	21.7
Electron Bunch Pulse rms temporal duration $\sigma_{t,\rm ele}$ (fs)		24			24	

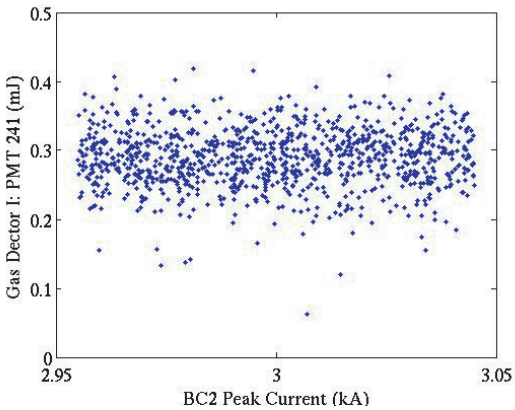

Figure 2: The distribution of the FEL energy vs. the electron bunch peak current in the final bin with 1028 measurement events.

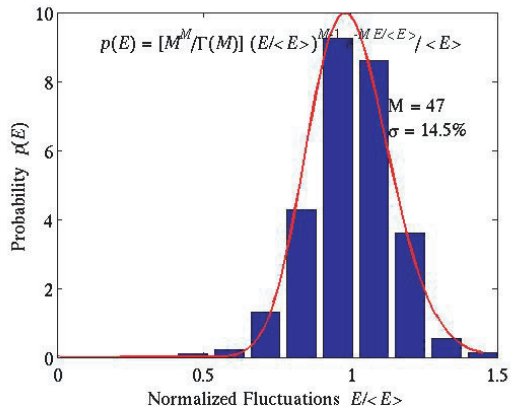

Figure 3: The final probability distribution $p(E)$ as function of the FEL energy in the final bin with 1028 measurement events.

above mentioned parameter set, the spike temporal duration $\tau_{\rm spike} = 295$ as. Hence, the FEL pulse temporal FWHM duration is $\tau_{\rm FEL} = 14$ fs, which should be compared to $\sigma_{t,\rm ele} = 24$ fs mentioned above. The FEL pulse temporal duration is shorter than the electron bunch temporal duration. To shed light on it, we perform a start-to-end simulation. The FEL pulse as the green spikes and the electron bunch current profile as the blue curve are shown in Fig. 4. The FEL pulse temporal duration is shown shorter than the electron bunch temporal duration. Fitting the FEL pulse spikes to an envelope Gaussian profile (the red curve) gives the FEL pulse FWHM of about 38 fs compared to the electron bunch FWHM of 83 fs.

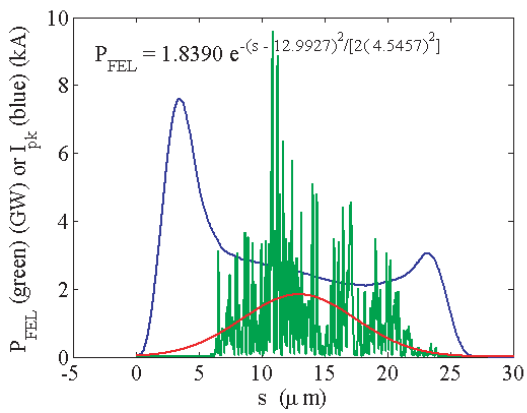

Figure 4: The simulated FEL pulse is shown as the green spikes and the simulated electron bunch current profile as the blue curve. The red curve is fitting the FEL pulse to a Gaussian distribution function.

Modes Number for Different Undulator Length In another experiment, we set the electron centroid energy at 14.233 GeV, so that the FEL is about 9 keV. The electron bunch peak current is set at $I_{pk} = 3$ kA, and with $\varepsilon_n = 0.6$ mm-mrad for both x- and y-plane, and absolute slice energy rms spread of $\sigma_E = 1.3$ MeV. The simulated gain length is $L_G \approx 3.31$ m. For measurements with undulator segments of 8 - 23 and 4 - 23, the undulator taper is again compensating for the spontaneous emission, the wakefield, and the FEL gain induced energy loss. We set the electron bunch for both under- and over-compressed cases with the peak current set at 3 kA for all the cases. For the measurements with undulator segments 1 - 23, there is additional post saturation quadratic tapering. The results are summarized in Table 2. Even though the theory does not apply to the deep saturation regime, we list the analysis for 23 undulator segments (1 - 23) case as a comparison. In general, it seems that the FEL pulse becomes longer when it approaches the saturation point as in Table 2. Again, we see a shorter FEL pulse than the electron bunch, which indicates local non-uniformity of the electron bunch in 6-D phase space. Since the FEL is extremely sensitive to the 6-D phase space parameters, the FEL starts and grows dif-

Table 3: Modes Number for 40 pC and 800 eV FEL Case ("L.T." stands for linear taper, "P.S.T." for post saturation taper).

	Undercompression			Overcompression			
Undulator Numbers	15-23	13-23	1-23	15-23	13-23		1-23
Undulator Taper	L.T.		P.S.T.	L.T.			P.S.T.
Peak Current (estimated)	8 kA			5 kA	4 kA	5 kA	
Modes Numbers	2	3	62	2	4	3	22

ferently at different parts of the electron bunch. The well-favored ones generate FEL dominating other parts, which makes the effective electron bunch shorter than the entire electron bunch.

Table 4: Modes Number for 20 pC and 800 eV FEL Case

	Undercomp.	**Overcomp.**
Undulator Segments	15-23	
Undulator Taper	Linear Taper	
Peak Current (estimated)	4 kA	
Modes Number	4	5

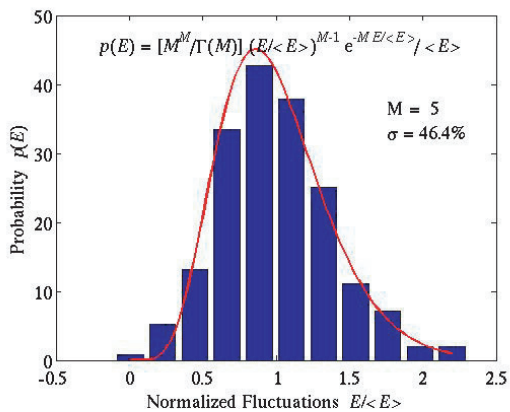

Figure 5: The FEL energy fluctuation indicates five modes in the FEL pulse for 20 pC, 800 eV FEL.

Experiments: Low Charge (40 pC and 20 pC)

For the low charge case, the bunch length monitor is no longer able to report accurate measurement of the electron bunch peak current after compression. However, the statistics approach described above for the 250 pC case can still be used in principle. The results are assembled for the 40 pC case in Table 3. As yet another example, the results are assembled for the 20 pC case in Table 4. For the 40 pC case, we also show the FEL pulse duration as a function of the undulator length. Again, it seems that the FEL pulse duration gets longer along the undulator. As an example, shown in Fig. 5, for the 20 pC charge with 800 eV FEL case in Table 4, there are about five modes in the FEL pulse. This is cross checked with spectrometer as shown in Fig. 6 showing only a few spikes in the frequency domain.

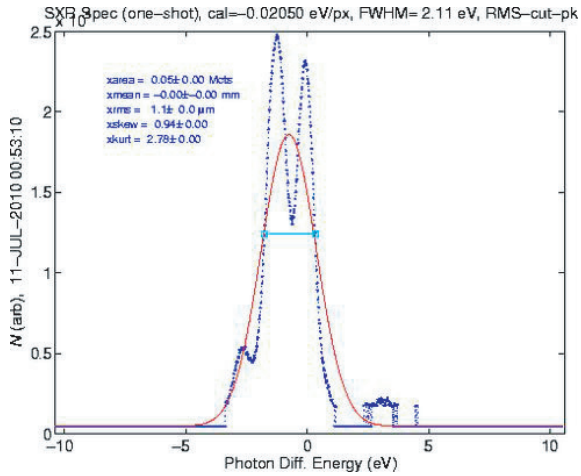

Figure 6: The spectrometer also indicates a few modes only in the FEL pulse for 20 pC, 800 eV FEL.

Discussion

The FEL pulse energy fluctuation measurements are conducted for various machine configuration. The results seem to indicate a shorter FEL pulse than the electron bunch, which may suggest local non-uniformity in the electron bunch 6-D phase space distribution. More detailed study is on-going to make this approach as a mature method to measure FEL pulse duration for LCLS. The authors thank J. Hastings, J. Krzywinski, G. Stupakov of SLAC, and C. Pellegrini of UCLA for fruitful discussions.

REFERENCES

[1] L. D. Smullin and H. A. Haus, *Noise in Electron Devices* (Wiley, NY, 1959).

[2] P. Catravas *et al.*, Phys. Rev. Lett. **82**, 5261 (1999).

[3] M. Hogan *et al.*, Phys. Rev. Lett. **80**, 289 (1998).

[4] W. Ackermann *et al.*, Nature Photonics, **1**, 336 (2007).

[5] P. Emma *et al.*, Nature Photonics, 2010 (published online: 1 Aug 2010 — DOI: 10.1038/NPHOTON.2010.176).

[6] E.L. Saldin, E.A. Schneidmiller, M.V. Yurkov, Optc. Commun. **148**, 383 (1998).

[7] L.H. Yu and S. Krinsky, NIMA **407**, 261 (1998); S. Krinsky, R.L. Gluckstern, NIMA **483**, 57 (2002).

[8] J.-M. Wang and L.-H. Yu, NIMA **250**, 484 (1986).

[9] K.J. Kim, NIMA **250**, 396 (1986); PRL **57**, 1871 (1986).